Calculation of Bearing Capacity of Fiberglass Grid Reinforced Asphalt Mixture Based on Stress-Strain Relationship

Yangjun Meng^{1,2,*}, Can Li³

¹School of Intelligent Architecture, Changde College, Changde, Hunan, China
²School of civil engineering and architecture, Hunan University of Arts and Science, Changde, Hunan, China
³Department of Engineering and Technology of Furong College, Hunan University of Arts and Science, Changde, Hunan, China
*Corresponding Author.

Abstract:

It can effectively reduce the damage of the asphalt mixture for bridge deck pavement to lay fiberglass grid in the asphalt mixture bridge deck pavement. However, there is little research on the bearing capacity of reinforced grid asphalt mixtures. Therefore, based on the material constitutive relationships and the plane section assumption, some relevant researches is conducted. Firstly, it is clear that the compression process of asphalt mixture can be divided into four stages, which are reverse bending stage, linear stage, hyperbolic stage, and failure stage. The stress-strain fitting formulas for each stage are different, and the stress on asphalt mixture bridge deck pavement is generally in the hyperbolic stage. Secondly, based on the assumption of plain section, the bearing capacity calculation formula for a double reinforced rectangular section with fiberglass grid reinforcement is derived by considering the compression and tension of the asphalt mixture separately. Finally, with specific examples, the correctness of the formula is verified. Meanwhile, in order to uniquely determine the area of fiberglass grid and steel reinforcement, we need to add an additional condition, usually with the lowest cost as the supplementary condition. Moreover, considering the stress effect of asphalt mixture and the effect of fiberglass grid reinforcement, a height of the compression zone of section is slightly reduced, and the structural bearing capacity is slightly improved.

Keywords: asphalt mixture, stress-strain relationship, fiberglass grid, reinforcement, bearing capacity

INTRODUCTION

Currently, asphalt mixture bridge deck pavement is widely used. After a period of operation, the damage to the asphalt mixture bridge deck pavement cannot be ignored. Therefore, Meng et al.[1] have proposed a method of overlaying a glass fiber grid on the asphalt mixture bridge deck pavement layer to improve the mechanical properties and durability of the asphalt mixture, which has yielded good results. Existing studies include: Li et al.[2] established a damage constitutive relationship considering the freeze-thaw effect of asphalt mixture based on the strain equivalence principle and Weibull distribution, and analyzed the impact of freeze-thaw cycles on the mechanical properties of asphalt mixtures in conjunction with uniaxial compression tests of asphalt mixtures under freeze-thaw cycle conditions. Gardezi et al.[3] increased the utilization of plastic ash composites (PAC) and RAP in hot mix asphalt (HMA) by changing their weight percentages in the mixture, while developing a complex machine learning method for gene expression programming (GEP) to predict their rut depth. Zhang and Li[4] conducted indirect tensile fatigue tests and established a viscoelastic-plastic damage constitutive model of asphalt mixtures considering the characteristics of dynamic cyclic loading and the influence of loading frequency. Adwani et al.[5] evaluated the influence of three commonly used WMA additives in India, namely Sasobit, Evotherm and Zycotherm, and basic adhesive VG-30 on the rheological properties and mixture performance parameters of asphalt mixtures. Xiao et al. [6] analyzed the time-temperature dependency of the mechanical properties of three types of asphalt mixtures and established master curves for different mechanical parameters. Hu et al.[7] conducted a study on the accuracy of time-temperature equivalence factors for master curves. Fan et al.[8] prepared rotarycompacted specimens of two types of modified asphalt mixtures, conducted performance tests, and determined the master curves of dynamic modulus for the two modified asphalt mixtures. Yin and Zhang[9] conducted dynamic creep experiments on four types of asphalt and two types of asphalt mixtures, fitted the creep curves of asphalt mixtures using the classical Burgers model and a fractional derivative Burgers model composed of a series combination of Maxwell body and fractional Kelvin body. Raza and Sharma[10] conducted research on PAM using systematic experiments and modeling methods such as response surface methodology (RSM) and artificial neural networks (ANN) to establish new, low experiment based guidelines for establishing a relationship between porosity and permeability while ensuring the stability of the mixture. Mahdi et al. [11] evaluated the potential of using geosynthetics to reinforce flexible pavements and improve their resistance to reflective cracking. Gou et al.[12] conducted triaxial tests on asphalt concrete and fitted the stress-strain curves using an improved hyperbolic model. Zheng et al.[13] conducted experimental research on the stress relaxation characteristics of asphalt mixtures under different temperature conditions, and analyzed and parameter-fitted the experimental results using the time-temperature equivalence principle of thermorheologically simple materials. Wu and Ma[14] summarized that the stress-strain curve can be divided into an antibending section, a linear section, a hyperbolic section, and a failure section, with a peak strain of around 0.004. Pratap et al.[15] researched the use of WMA technology to minimize the production temperature of rubber particle modified (CRM) adhesives. Wang et al.[16] proposed a new method for calculating the tangent modulus using a modified Duncan-Chang hyperbolic model, a new method for calculating the tangent Poisson's ratio using a modified Deniels formula, and a new failure criterion for asphalt concrete materials. Ye [17] studied the mechanical properties of thin overlay asphalt mixtures based on the discrete element method. Suleiman et al.[18] investigated the Dynamic Creep of Polymer Modified Hot Mix Asphalt. Wang and Wu[19] prepared compression specimens of asphalt concrete and conducted stress-strain experimental studies. Vaibhav et al.[20] conducted a comprehensive study on the performance evaluation of modified binders and warm mix asphalt (WMA) in open graded friction layer (OGFC) and stone based asphalt (SMA) mixtures.

In summary, although there is substantial research on asphalt mixtures, but there is relatively little research on grid reinforced asphalt mixture bridge deck pavement, and the research is scattered and lacks relevant standards. Therefore, it is necessary to conduct research on the bearing capacity of reinforced asphalt mixtures, which has significant practical implications for guiding engineering practice.

OVERVIEW OF THE STRESS-STRAIN RELATIONSHIP OF ASPHALT MIXTURES

There is limited research on the stress-strain relationship of asphalt mixtures, primarily concentrated in the 1990s to around the year 2000. The research typically used cylindrical specimens and focused on triaxial experiments to study the relationship between deviatoric stress (σ_1 - σ_3) and axial strain (ε_1).

Through analysis and summarization, the compression process of asphalt mixtures can be divided into the following stages (Figure 1): ① Reverse bending segment OA: The specimen is initially compressed, and due to pore compression, the stress-strain curve shows a reverse bending point A. The tangent modulus at the origin is E_0 , and the secant modulus for segment OA is E_1 . ② Linear segment AE: The stress-strain relationship is linear, and the linear elastic modulus is E_1 . ③ Hyperbolic segment EBD: The stress-strain relationship follows a curve, with point B corresponding to the maximum volumetric strain point B', and point D where the stress reaches its maximum value. The tangent modulus for segment EBD is E_1 . ④ Failure segment DCF: The stress decreases to the volumetric recovery point C', the stress drops rapidly, and the specimen undergoes macroscopic volume expansion until failure.

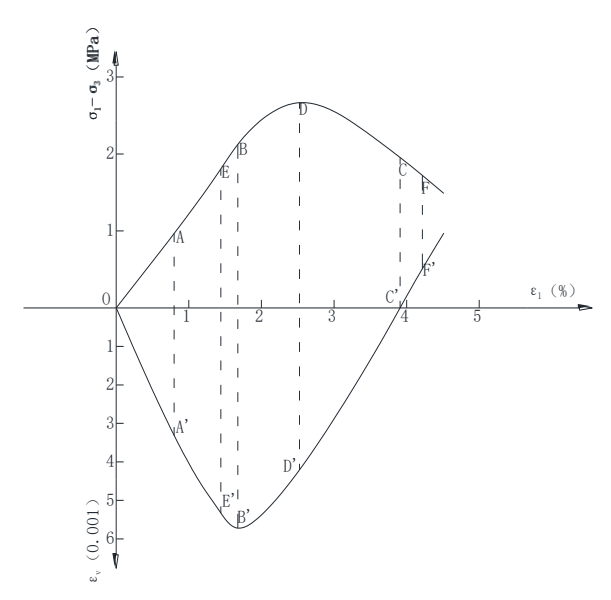


Figure 1. Stress-strain curve and volumetric strain curve of asphalt mixture

Upon reviewing existing literature, no expression for the stress-strain relationship of asphalt mixtures was found. Based on the data from Reference [12] (Table 1), a fitted stress-strain relationship curve for asphalt mixtures was obtained, as shown in Table 2 and Figure 2.

Since point E is not a special point and cannot be directly read during the experiment, it must be solved for during curve fitting segmentation. The specific solution method is as follows: Assuming that the stress-strain relationship for the hyperbolic segment

satisfies $s = \frac{e}{A + Be}$ [10], and knowing that the curve passes through points B and D, parameters $A = \frac{\varepsilon_{\rm B}\varepsilon_{\rm D}}{\varepsilon_{\rm B} - \varepsilon_{\rm D}} \left(\frac{1}{\sigma_{\rm D}} - \frac{1}{\sigma_{\rm B}}\right)$ and

 $B = \frac{1}{\varepsilon_{\rm B} - \varepsilon_{\rm D}} \left(\frac{\varepsilon_{\rm B}}{\sigma_{\rm B}} - \frac{\varepsilon_{\rm D}}{\sigma_{\rm D}} \right)$ can be obtained; since point E is on the linear segment, the slope of segment AE equals the linear elastic

modulus $E_{\rm II}$. Solving the simultaneous equations $E_{\rm II} = \frac{\sigma_{\rm E} - \sigma_{\rm A}}{\varepsilon_{\rm E} - \varepsilon_{\rm A}}$, $\sigma_{\rm E} = \frac{\varepsilon_{\rm E}}{a + b\varepsilon_{\rm E}}$, $\varepsilon_{\rm E}$ and $\sigma_{\rm E}$ can be calculated.

Table 1. Triaxial experimental data of asphalt mixture

1	2	3
3.91	3	2.12
1.43	0.81	0.65
0.72	0.69	0.55
2.83	2	1.29
1.31	1.76	1.84
3.55	2.6	1.85
1.51	2.42	3.05
168.8	112.8	113.6
a) 198.6	117.4	118.2
307.8	155.2	130.1
	1.43 0.72 2.83 1.31 3.55 1.51 168.8 a) 198.6	1.43 0.81 0.72 0.69 2.83 2 1.31 1.76 3.55 2.6 1.51 2.42 168.8 112.8 a) 198.6 117.4

Table 2. Stress strain relationship fitting curves of asphalt mixture

Specimen number	Stages	Fitting curves
1	Reverse bending segment:	$\sigma - 1.43 = \left(168.8 + 139.0 \frac{i}{n}\right) \frac{\varepsilon - 0.72}{100}, \ \varepsilon \in \left(0, 0.72\right)$
	Linear segment:	$\sigma - 1.43 = 307.8 \times \frac{\varepsilon - 0.72}{100}, \varepsilon \in (0.72, 0.80)$
	Hyperbolic segment:	$\sigma = \frac{\varepsilon}{0.70882 - 0.18773\varepsilon}, \varepsilon \in (0.80 , 1.51)$
2	Reverse bending segment:	$\sigma - 0.81 = \left(112.8 + 42.4 \frac{i}{n}\right) \frac{\varepsilon - 0.69}{100}, \varepsilon \in \left(0, 0.69\right)$
	Linear segment:	$\sigma - 0.81 = 155.2 \times \frac{\varepsilon - 0.69}{100}, \varepsilon \in (0.69, 0.70)$
	Hyperbolic segment:	$\sigma = \frac{\varepsilon}{0.744615 + 0.076923\varepsilon}, \varepsilon \in (0.70 , 2.42)$
3	Reverse bending segment:	$\sigma - 0.65 = \left(113.6 + 16.5 \frac{i}{n}\right) \frac{\varepsilon - 0.55}{100}, \ \varepsilon \in \left(0, 0.55\right)$
	Linear segment:	$\sigma - 0.65 = 130.1 \times \frac{\varepsilon - 0.55}{100}, \varepsilon \in (0.55, 0.56)$
	Hyperbolic segment:	$\sigma = \frac{\varepsilon}{1.088326 + 0.183712\varepsilon}, \varepsilon \in (0.56 , 3.05)$

Note: The units of σ , ε in the table are MPa and 1/100, respectively. The "n" represents the number of segments of the fitted curve in the reverse bending segment, and "i" is the number of segments. Take the extension of the hyperbolic segment as the destructive segment.

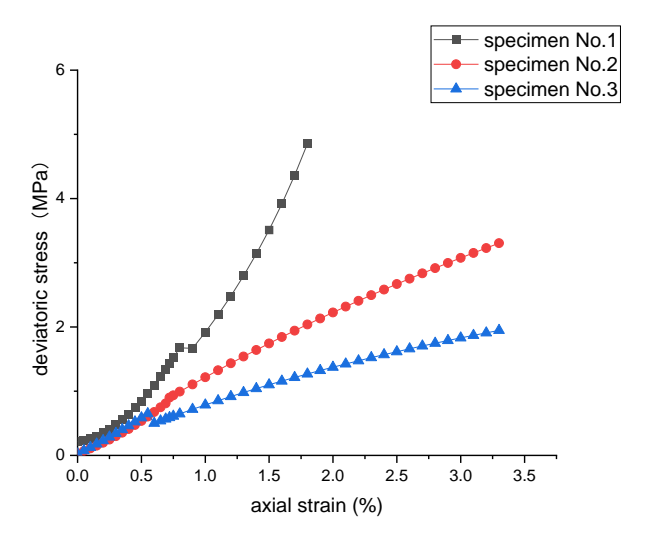


Figure 2. Stress-strain fitting curve of asphalt mixture

CALCULATION THEORY AND METHOD

Reinforced asphalt mixture bridge deck pavement is generally carried out after the construction of main structure of the bridge. For the permanent load effects, the asphalt mixture pavement layer only bears the secondary dead load such as its own weight; variable loads and accidental effects are shared with the main structure.

Taking the reinforced asphalt mixture bridge deck pavement on a double-reinforced rectangular concrete section as an example, we do not consider the tensile strength of concrete and the viscoelastic effects of the asphalt mixture, the bearing capacity of fiberglass grid reinforced asphalt mixture have been analyzed.

Compression of the Asphalt Mixture Layer

Under the combined action of bending moment M and axial force N, the calculation diagram of the normal section bearing capacity is shown in Figure 3, where the strain distribution across the section exhibits a double curve distribution pattern.

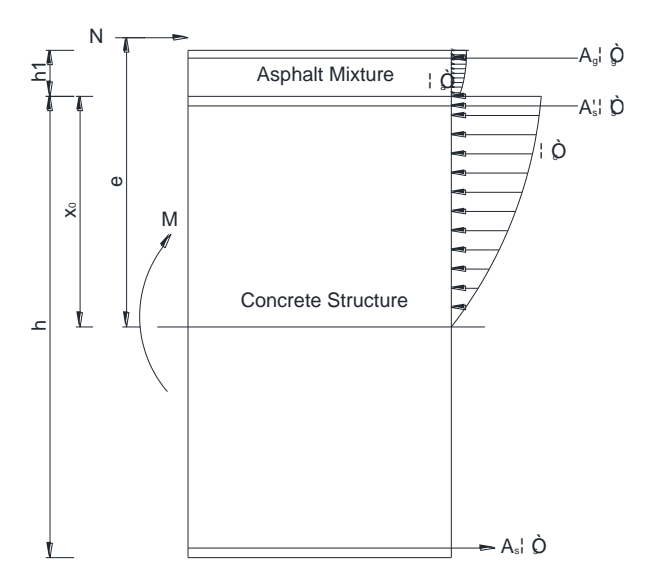


Figure 3. Calculation diagram of normal section bearing capacity (Asphalt mixture under compression)

The constitutive relationship for concrete follows the "Code for Design of Concrete Structures" (GB 50010-2010) (2015 edition):

$$\sigma_{c} = f_{c} \left[1 - (1 - \frac{\varepsilon_{c}}{\varepsilon_{0}})^{2} \right], \varepsilon_{c} \leq \varepsilon_{0}$$

$$\sigma_{c} = f_{c}, \varepsilon_{0} < \varepsilon_{c} \leq \varepsilon_{cu}$$
(1)

Taking into account the concrete strength of the bridge structures, ε_0 =0.002, ε_{cu} =0.0033.

Statistical analysis indicates that most working states (stress-strain curves) of the asphalt mixture bridge deck pavement fall within the hyperbolic segment. At this stage, the stress-strain relationship satisfies the Duncan-Chang model, as shown in Equation (2):

$$s = \frac{e}{A + Be} \tag{2}$$

Where σ and ε represent the axial stress and strain of the asphalt mixture, respectively, while A and B are parameters to be determined.

Based on the principles of elastic mechanics, the strain of the compressed region of concrete (or asphalt mixture) is given by:

$$\varepsilon = \frac{x}{\rho} \tag{3}$$

Where ρ is the curvature of the section, and x is the distance from the neutral axis O_c to the concrete (or asphalt mixture) in the compressed region.

According to the section equilibrium condition, we obtain:

$$N = \int_{0}^{x_{0}} \sigma_{c} dA + \int_{x_{0}}^{x_{0} + h_{1}} \sigma_{a} dA + A'_{s} \sigma'_{s} - A_{s} \sigma_{s} + A_{g} \sigma_{g}$$
(4)

$$M + Ne = \int_{0}^{x_0} \sigma_c x dA + \int_{x_0}^{x_0 + h_1} \sigma_a x dA + A_s \sigma_s (h - a_s - x_0) + A_s' \sigma_s' (x_0 - a_s') + A_g \sigma_g (x_0 + h_1 - a_g)$$
 (5)

Where A_s and A'_s represent the areas of steel reinforcement in the tensile and compressive regions of the concrete, respectively; σ_s and σ'_s represent the tensile and compressive stresses of the steel reinforcement, respectively; a_s and a'_s represent the distances from the resultant force point of the steel reinforcement in the tensile and compressive regions to the edges of the tensile and compressive regions of the concrete, respectively; A_g , σ_g , and a_g represent the area, stress, and distance from the resultant force point of the tensile reinforcement grid to the edge of the asphalt mixture in the tensile region, respectively; x_0 represents the height of the compressed region of concrete; h and h_1 represent the heights of the concrete section and the asphalt mixture section, respectively.

Considering the linear distribution of strain in the asphalt mixture layer, substituting Equation (1a) into Equation (4) gives:

$$N = \int_{0}^{x_{0}} \left(E_{1} \frac{x}{\rho} - E_{2} \frac{x^{2}}{\rho^{2}} \right) b dx + \int_{x_{0}}^{x_{0} + h_{1}} \left[\frac{x/\rho}{A + B x/\rho} \right] b dx + A'_{s} \sigma'_{s} - A_{s} \sigma_{s} + A_{g} \sigma_{g}$$
 (6)

Analyzing and organizing gives:

$$N = b \left(E_1 \frac{x_0^2}{2\rho} - E_2 \frac{x_0^3}{3\rho^2} \right) + N_1 + N_0$$
 (7)

Where b is the width of rectangular cross-section, $E_1 = \frac{2f_c}{\varepsilon_0}$, $E_2 = \frac{f_c}{\varepsilon_0^2}$, $N_0 = A_s'\sigma_s' - A_s\sigma_s + A_g\sigma_g$,

$$N_{1} = \frac{b\left(A\rho \ln \frac{A\rho + Bx_{0}}{A\rho + B(x_{0} + h_{1})} + Bh_{1}\right)}{B^{2}}.$$

Substituting Equation (1a) into Equation (5), analyzing and organizing gives:

$$M + Ne = b \left(E_1 \frac{x_0^3}{3\rho} - E_2 \frac{x_0^4}{4\rho^2} \right) + M_1 + N_0 x_0 + M_0$$
 (8)

Where
$$M_0 = A_s \sigma_s h_0 - A_s' \sigma_s' a_s' + A_g \sigma_g (h_1 - a_g)$$
, $M_1 = \frac{b\{A^2 \rho^2 \ln \frac{A\rho + B(x_0 + h_1)}{A\rho + Bx_0} - Bh_1 \left[A\rho - B(x_0 + \frac{h_1}{2})\right]\}}{B^3}$.

The above derivation is based on the limit equilibrium state of the section, where the tensile reinforcement yields and the concrete at the compressive edge reaches the ultimate strain ε_{cu} . That is:

$$\varepsilon_{\rm cu} = \frac{x_0}{\rho} \tag{9}$$

Substituting Equation (9) into Equations (7) and (8), organizing gives:

$$N = b \left(\frac{E_1 \varepsilon_{cu}}{2} - \frac{E_2 \varepsilon_{cu}^2}{3} \right) x_0 + \frac{b \left[A \frac{x_0}{\varepsilon_{cu}} \ln \frac{A x_0 + x_0 B \varepsilon_{cu}}{A x_0 + B \left(x_0 + h_1 \right) \varepsilon_{cu}} + B h_1 \right]}{B^2} + N_0$$

$$(10)$$

$$N(e + e_a) = b\left(\frac{E_1 \varepsilon_{cu}}{3} - \frac{E_2 \varepsilon_{cu}^2}{4}\right) x_0^2 + \frac{b\{A^2 \frac{x_0^2}{\varepsilon_{cu}^2} \ln \frac{Ax_0 + B(x_0 + h_1)\varepsilon_{cu}}{Ax_0 + x_0 B\varepsilon_{cu}} - Bh_1 \left[A \frac{x_0}{\varepsilon_{cu}} - B\left(x_0 + \frac{h_1}{2}\right)\right]\}}{B^3} + N_0 x_0 + M_0$$
(11)

Equations (10) and (11) are the calculation formulas for the normal section bearing capacity of grid reinforced asphalt mixture bridge deck pavement. At this time:

$$\frac{\varepsilon_{s} + \varepsilon_{cu}}{\varepsilon_{cu}} = \frac{f_{y}/E_{s} + \varepsilon_{cu}}{\varepsilon_{cu}} = \frac{h_{0}}{x_{0b}}$$
(12)

$$\frac{\varepsilon_g + \varepsilon_{cu}}{\varepsilon_{cu}} = \frac{f_g / E_g + \varepsilon_{cu}}{\varepsilon_{cu}} = \frac{x_0 + h_1 - a_g}{x_0}$$
(13)

Here $h_0=h-a_s$.

Calculation and analysis show that the height of the compressed region of concrete $x_{0b} = \frac{\mathcal{E}_{cu}}{f_y/E_s + \mathcal{E}_{cu}} h_0$, when $\varepsilon_{\text{cu}} = 0.0033 f_y = 360 \text{MPa}$, $E_s = 2.0 \times 10^5 \text{MPa}$, when $E_s = 2.0 \times 10^5 \text{MPa}$, $E_s = 2.0 \times 10^5 \text{MPa}$, when $E_s = 2.0 \times 10^5 \text{MPa}$, $E_s = 2.0 \times 10^5 \text{MPa}$, when E_s

Tension in the Asphalt Mixture Layer

Under the combined action of bending moment M and axial force N, the calculation diagram for the normal section bearing capacity is shown in Figure 4, where the strain distribution across the section exhibits a curve distribution pattern. For safety considerations, the tensile effect of the asphalt mixture is not taken into account.

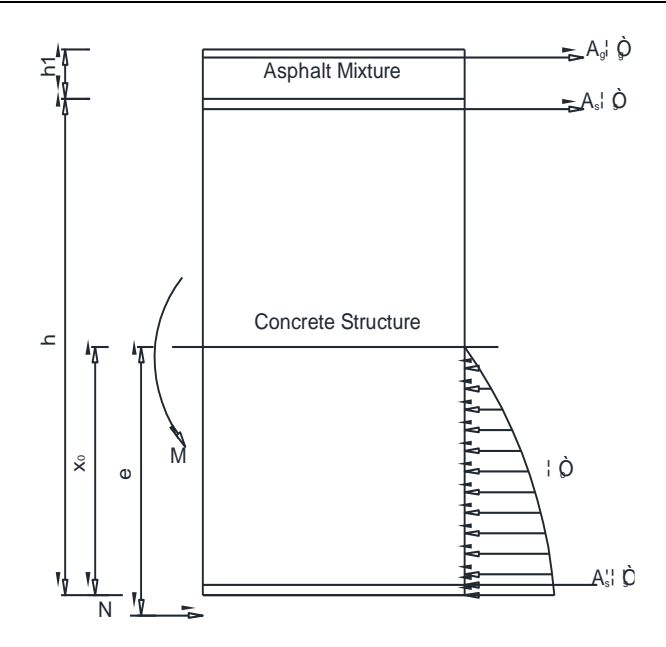


Figure 4. Calculation diagram of normal section bearing capacity (Asphalt mixture under tension)

Following the same analysis, according to the section equilibrium condition, we obtain:

$$N = \int_0^{x_0} \sigma_c dA + A_s' \sigma_s' - A_s \sigma_s - A_g \sigma_g$$
 (14)

$$M + Ne = \int_{0}^{x_0} \sigma_{c} x dA + A_{s} \sigma_{s} (h - a_{s} - x_0) + A'_{s} \sigma'_{s} (x_0 - a'_{s}) + A_{g} \sigma_{g} (h + h_1 - x_0 - a_{g})$$
(15)

Analyzing and organizing gives:

$$N = b \left(E_1 \frac{x_0^2}{2\rho} - E_2 \frac{x_0^3}{3\rho^2} \right) + N_0 \tag{16}$$

$$M + Ne = b \left(E_1 \frac{x_0^3}{3\rho} - E_2 \frac{x_0^4}{4\rho^2} \right) + N_0 x_0 + M_0$$
 (17)

Where
$$N_0 = A_s'\sigma_s' - A_s\sigma_s - A_e\sigma_e$$
, $M_0 = A_s\sigma_s h_0 - A_s'\sigma_s' a_s' + A_e\sigma_e (h + h_1 - a_e)$.

The above derivation is still based on the limit equilibrium state of the section, where the tensile reinforcement yields and the concrete at the compressive edge reaches the ultimate strain ε_{cu} . Analyzing and organizing gives:

$$N = b \left(\frac{E_1 \varepsilon_{cu}}{2} - \frac{E_2 \varepsilon_{cu}^2}{3} \right) x_0 + N_0$$
 (18)

$$N(e + e_a) = b \left(\frac{E_1 \varepsilon_{cu}}{3} - \frac{E_2 \varepsilon_{cu}^2}{4} \right) x_0^2 + N_0 x_0 + M_0$$
 (19)

When applying Equations (10) and (11), Equations (18) and (19), it is important to note the stress-strain relationship of concrete: when $\varepsilon_0 < \varepsilon_c \le \varepsilon_{cu}$, the stress of the concrete is $\sigma_c = f_c$, and the corresponding stress of the reinforcement σ_s is given when $\varepsilon_s > f_y / E_s$, $\sigma_s = f_y$. Combined with the section equilibrium condition, the formulas are slightly modified.

CALCULATION EXAMPLES

In order to verify the correctness of the above formulas, a double-reinforced rectangular section beam is chosen for validation.

Pure Bending Rectangular Section

Given $b \times h = 250 \text{mm} \times 500 \text{mm}$, M = 210 kN.m (tension at the bottom of the beam), Class I environment, C30, $f_c = 14.3 \text{MPa}$, 2C20 reinforcement in the compressive zone, $\varepsilon_0 = 0.002$, $\varepsilon_{cu} = 0.0033$, calculate the area of tensile reinforcement A_s .

First, Ignore asphalt mixture bridge deck pavement. Referring to the "Specifications for Design of Highway Reinforced Concrete and Prestressed Concrete Bridges and Culverts" (JTG 3362-2018), the minimum thickness of the concrete cover for the beam is 20 mm, taking h_0 =35mm. Using the method described in this paper:

$$E_1 = \frac{2f_c}{\varepsilon_0} = 1.43 \times 10^4 \text{ MPa}$$
, $E_2 = \frac{f_c}{\varepsilon_0^2} = 3.575 \times 10^6 \text{ MPa}$, $x_{0b} = 0.647 h_0 = 300.9 \text{ mm}$, $2a_s = 70 \text{ mm}$.

Equations (10) and (11) are transformed into:

$$250 \times \left(\frac{1.43 \times 10^4}{2} \times 0.0033 - \frac{3.575 \times 10^6}{3} \times 0.0033^2\right) x_0 + 360 \times 2 \times \frac{\pi \times 20^2}{4} - 360 A_s = 0$$

$$250 \times \left(\frac{1.43 \times 10^4}{3} \times 0.0033 - \frac{3.575 \times 10^6}{4} \times 0.0033^2\right) x_0^2 + \left(360 \times \frac{2\pi \cdot 20^2}{4} - 360A_s\right) x_0 + 360A_s \cdot 465 - 360 \times \frac{2\pi \cdot 20^2}{4} \times 35 = 2.1 \times 10^8$$

Simultaneously solving the above two equations gives $x_0=100.9$ mm($2a_s$ ' $< x_0 < x_{0b}$), $A_s=1372.0$ mm²(>0.2% $bh_0=232.5$ mm²).

Using the code method, $x_{0b}=0.518h_0=241$ mm, $2a_s'=70$ mm.

$$x = h_0 - \sqrt{h_0^2 - 2\left[\frac{M - f_y'A_s'(h_0 - a_s')}{\alpha_1 f_c b}\right]} = 465 - \sqrt{465^2 - 2\left[\frac{2.1 \times 10^8 - 360 \times \frac{2\pi \times 20^2}{4}(465 - 35)}{1.0 \times 14.3 \times 250}\right]} = 73.7 mm$$

$$A_s = \frac{\alpha_1 f_c bx}{f_v} + A_s' = \frac{1.0 \times 14.3 \times 250 \times 73.7}{360} + \frac{2\pi \times 20^2}{4} = 1360 \text{mm}^2$$

Through comparison and analysis, it is evident that the formulas derived in this paper are accurate and reliable.

Given the same data, considering a 10cm asphalt mixture bridge deck pavement, with glass fiber grid E_g =12.1GPa, and asphalt mixture stress-strain parameters A=0.744615, B=0.076923, calculate the area of tensile reinforcement A_s and the area of the reinforced grid A_g for the asphalt mixture.

Analyzing and organizing Equations (10) and (11) gives:

$$250 \times \left(\frac{1.43 \times 10^{4}}{2} \times 0.0033 - \frac{3.575 \times 10^{6}}{3} \times 0.0033^{2}\right) x_{0} + \frac{250}{B^{2}} \cdot \left(\frac{Ax_{0}}{0.0033} \ln \frac{Ax_{0} + 0.0033Bx_{0}}{Ax_{0} + B(x_{0} + 100) \times 0.0033} + 100B\right) + 360 \times 2 \times \frac{\pi \times 20^{2}}{4} - 360A_{s} + A_{g}\sigma_{g} = 0$$

$$250 \times \left(\frac{1.43 \times 10^{4}}{3} \times 0.0033 - \frac{3.575 \times 10^{6}}{4} \times 0.0033^{2}\right) x_{0}^{2} + \left(360 \times \frac{2\pi \times 20^{2}}{4} - 360A_{s} + A_{g}\sigma_{g}\right) x_{0} + \frac{250}{B^{3}} \times \left(4A^{2} + \frac{x_{0}^{2}}{0.0033^{2}} \ln \frac{Ax_{0} + 0.0033B(x_{0} + 100)}{Ax_{0} + 0.0033Bx_{0}} - 100B \times \left[\frac{Ax_{0}}{0.0033} - \left(x_{0} + \frac{100}{2}\right)B\right]\right) + 360A_{s} \times 465 - 360 \times \frac{2\pi \times 20^{2}}{4} \times 35 + A_{g}\sigma_{g}(100 - a_{g}) = 2.1 \times 10^{8}$$

Then, Considering the compressive effect of the asphalt mixture pavement layer without the reinforcement effect of the grid, i.e., A_g =0, simultaneously solving the above two equations gives x_0 =100.7mm ($2a_s$ '< x_0 < x_0), A_s =1371.5mm²(>0.2% bh_0 =232.5mm²).

At last, Considering the compressive effect of the asphalt mixture pavement layer and the reinforcement effect of the grid, combining Equation (13), the grid stress $\sigma_g = E_g \varepsilon_g = E_g \frac{h_1 - a_g}{x_0} \varepsilon_{cu}$ can be obtained, and substituting it into the above equations gives the relationship between the height of the compressive zone x_0 , A_s , and A_g . For details, see Figures 5 to 7.

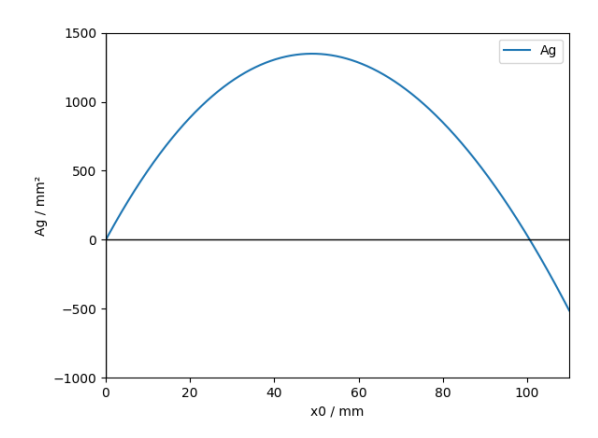


Figure 5. Relationship between the height of compression zone x_0 and the geogrid area

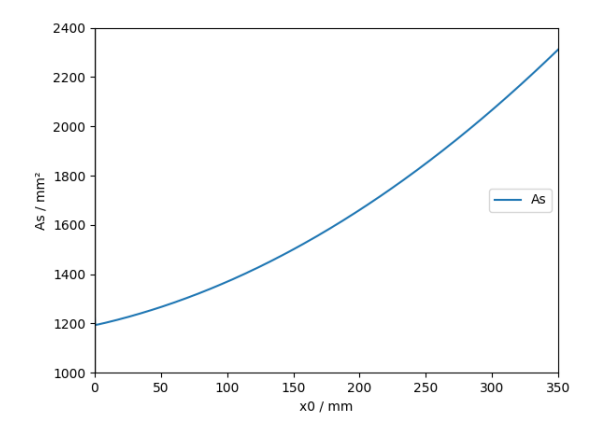


Figure 6. Relationship between the height of compression zone x_0 and the reinforcement area

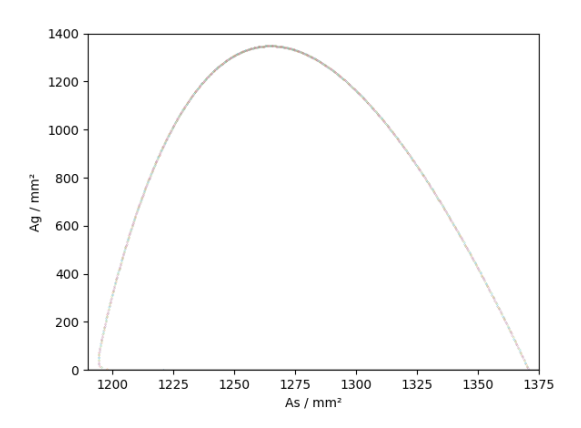


Figure 7. Relationship between reinforcement area and geogrid area

By solving, it was found that to uniquely determine the grid area and reinforcement area, an additional condition is required. Typically, the lowest cost can be used as the supplementary condition equation, which allows for the specific values of the reinforced grid area and reinforcement area to be obtained.

From Figures 5 to 7, it is not difficult to see that when considering the compression of the asphalt mixture layer, as the height of the compressed region increases, the grid area first increases and then decreases, while the reinforcement area increases with the increase in the height of the compressed region.

For a fixed height of the compressed region, there is a one-to-one relationship between the grid area and the reinforcement area. As the reinforcement area increases, the grid area first increases and then decreases. When the height of the compressed region

 $x_0 < 2a_s$, the grid stress calculated under the assumption of a plane section is too large, which does not conform to the actual situation. In practical applications, the section where $x_0 \ge 2a_s$ ' should be taken.

The analysis shows that considering the asphalt mixture bridge deck pavement, the height of the compressed region of the section slightly decreases, and the structural bearing capacity slightly increases. That is, under unchanged external loads (or effects), increasing the grid area can reduce the reinforcement area of the section.

Eccentrically Compressed Rectangular Section

A 10cm reinforced asphalt mixture bridge deck pavement (glass fiber grid E_g =12.1GPa, asphalt mixture stress-strain parameters A=0.744615, B=0.076923, E_a =4.0GPa) is laid on a rectangular reinforced concrete beam section. Given $b \times h$ =300mm \times 500mm,N=320kN, M_1 = -201kN.m (tension at the top of the beam), M_2 = -224kN.m (tension at the top of the beam), calculation length l_0 =2.4m. Class I environment, C30, f_c =14.3MPa, 4C20 reinforcement in the compressed zone. Calculate the area of tensile reinforcement A_s and the area of the reinforced grid A_g for the asphalt mixture.

Referring to the "Specifications for Design of Highway Reinforced Concrete and Prestressed Concrete Bridges and Culverts" (JTG 3362-2018), the minimum thickness of the concrete cover for the beam is 20mm, taking h_0 =35mm. Using the method described in this paper:

$$E_1 = \frac{2f_c}{\varepsilon_0} = 1.43 \times 10^4 \, \text{MPa} \qquad , \qquad E_2 = \frac{f_c}{\varepsilon_0^2} = 3.575 \times 10^6 \, \text{MPa} \qquad , \qquad x_{0b} = 0.647 h_0 = 300.9 \, \text{mm}, \qquad 2a_s = 70 \, \text{mm}, \qquad \frac{l}{i} = \frac{2.4}{0.5/\sqrt{12}} = 16.63 \leq 34 - 12 \frac{M_1}{M_2} = 34 - 12 \times \frac{201}{224} = 23.23 \, , \\ \text{Ignoring the second-order effect of axial force}. \qquad \qquad 2a_s = 70 \, \text{mm}, \qquad 2a_s = 70 \, \text$$

Equations (18) and (19) are transformed into:

$$300 \times \left(\frac{1.43 \times 10^{4}}{2} \times 0.0033 - \frac{3.575 \times 10^{6}}{3} \times 0.0033^{2}\right) x_{0} + 360 \times 4 \times \frac{\pi \times 20^{2}}{4} - 360 A_{s} - A_{g} \sigma_{g} = 320 \times 10^{3}$$

$$300 \times \left(\frac{1.43 \times 10^{4}}{3} \times 0.0033 - \frac{3.575 \times 10^{6}}{4} \times \right) x_{0}^{2} + \left(\frac{360 \times \frac{4\pi \times 20^{2}}{4} - 360 A_{s} - A_{g} - 360 A_{g} \times 465 - 360 \times \frac{4\pi \times 20^{2}}{4} \times 35 + A_{g} \sigma_{g} \times 500 + 100 - a_{g} \times 10^{2} \times 10^{2}$$

When the reinforcement effect of the grid is not considered, i.e., A_g =0, solving the equations gives x_0 =107.94mm ($2a_s$ '< x_0 < x_{0b}) A_s = 1322.84mm². Using the code formulas, the solution yields x_0 =62.3mm, A_s =1110.2mm², which belongs to large eccentric compression and does not satisfy $2a_s$ '< x_0 < x_0 b. Therefore, x_0 = $2a_s$ '=70mm, A_s =1201.3mm² should be taken.

Considering the reinforcement effect of the grid, based on the plane section assumption, the grid stress $\sigma_{\rm g} = E_{\rm g} \varepsilon_{\rm g} = E_{\rm g} \frac{h + h_{\rm l} - x_{\rm 0} - a_{\rm g}}{x_{\rm 0}} \varepsilon_{\rm cu}$ can be obtained, and substituting it into the above equations gives the relationship between

the height of the compressed region x_0 , A_s , and A_g . For details, see Figures 8 to 10.

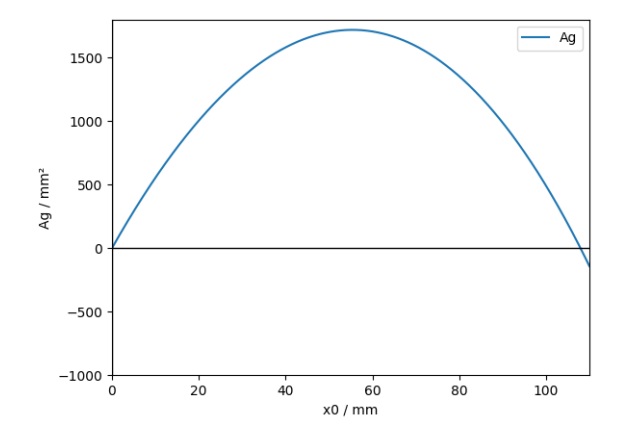


Figure 8. Relationship between the height of compression zone x_0 and the geogrid area

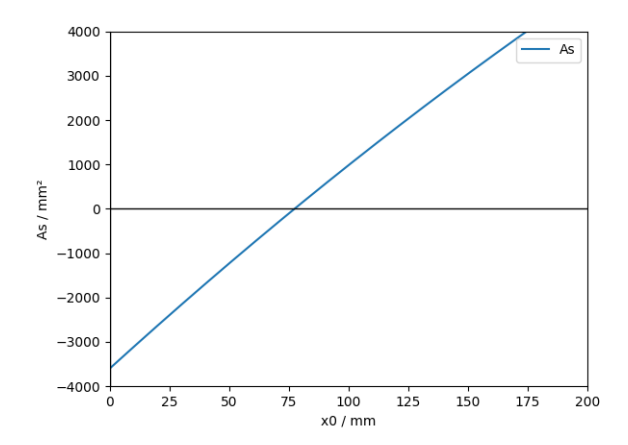


Figure 9. Relationship between the height of compression zone x_0 and the reinforcement area

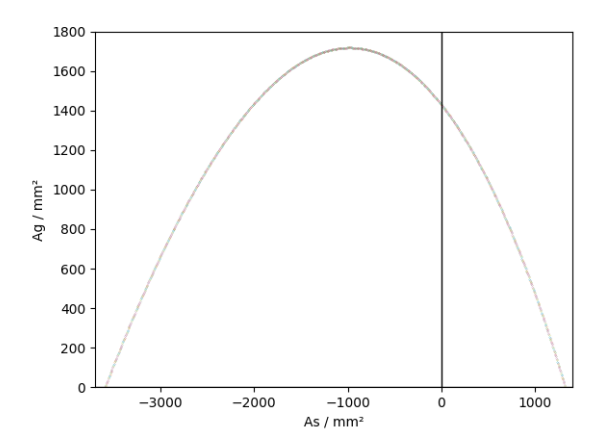


Figure 10. Relationship between reinforcement area and geogrid area

By solving, it was found that to uniquely determine the grid area and reinforcement area, an additional condition is required. Typically, the lowest cost can be used as the supplementary condition equation, which allows for the specific values of the reinforced grid area and reinforcement area to be obtained.

From Figures 8 to 10, it can be seen that when the tensile effect of the asphalt mixture layer is not considered, as the height of the compressed region increases, the grid area first increases and then decreases, while the reinforcement area increases with the increase in the height of the compressed region.

For a fixed height of the compressed region, there is a one-to-one relationship between the grid area and the reinforcement area. As the reinforcement area increases, the grid area first increases and then decreases. When the height of the compressed region $x_0 < 2a_s$, the grid stress calculated under the assumption of a plane section is too large, resulting in a negative value for the reinforcement area, which does not conform to the actual situation. In practical applications, the section where $x_0 \ge 2a_s$, should be taken.

The analysis shows that considering the effect of the reinforced grid, the height of the compressed region of the section slightly decreases, and the structural bearing capacity slightly increases. That is, under unchanged external loads (or effects), increasing the grid area can reduce the reinforcement area of the section.

CONCLUSIONS

The compression process of asphalt mixtures can be divided into four stages, and the stress on asphalt mixture bridge deck pavement falls within the hyperbolic stage. Considering the compression and tension of the asphalt mixture layer separately, based on the plane section assumption, the bearing capacity calculation formulas for a double-reinforced rectangular section with grid reinforcement were derived. To uniquely determine the grid area and reinforcement area, an additional condition is required.

To avoid an overly small compressed region, which would not be consistent with actual conditions, the portion where $x_0 \ge 2a_s$ ' should be taken in practical applications.

When considering the stress effect of the asphalt mixture and the reinforcement effect of the grid, the structural bearing capacity slightly increases. To ensure the normal and stable operation of the structure and meet construction requirements, it is recommended to lay a layer of EGA 60kN-60kN glassfiber grid on the asphalt mixture pavement in the project.

Laying fiberglass grid in the asphalt mixture bridge deck pavement can effectively reduce the damage of the asphalt mixture for bridge deck pavement, Therefore, conducting research on it has strong practical value. Looking forward, further research is needed on the composition, mechanism of action, and especially the mechanical properties considering the viscoelastic effect of grid reinforced asphalt mixtures.

ACKNOWLEDGEMENT

This research was supported by the Hunan Provincial Natural Science Foundation Project (2021JJ50136).

REFRENCES

- [1] Meng Yangjun, Liu Zhen, Liu Guojun, Wu Wenbiao, Liu Xiaofeng. Experimental research on performance of concrete bridge deck pavement with grid reinforced asphalt mixture. Sichuan Cement, 2023, (04):247-251.
- [2] Li Ping, Zhao Junlin, Lian Tengfei, Wang Xiaobo. Research on damage constitutive relationship of continuous dense gradation asphalt mixture under freeze thaw cycles. Engineering journal of Wuhan University, 2023, 56(03): 314-321.
- [3] Gardezi H, Ikrama M, Usama M, et al. Predictive modeling of rutting depth in modified asphalt mixes using gene-expression programming (GEP): A sustainable use of RAP, fly ash, and plastic waste. Construction and building materials, 2024, 443137809-137809.
- [4] Zhang Jun, Li Zhiwei. Viscoelastic-Plastic damage constitutive model of asphalt mixture under cyclic loading. Journal of Northeastern University (Natural Science), 2019,40(10):1496-1503.
- [5] Adwani D, Kumar P, Sharma A, et al. Comprehensive rheological and mechanistic evaluation of an asphalt binder and mixture modified with warm mix additives. Environmental Science and Pollution Research, 2024, (prepublish):1-14.
- [6] Xiao Yue, Li Libin, Li Qiang. Time temperature dependency of mechanical parameters for asphalt mixtures. Shan Xi Architecture, 2013, 39(26):92-94.
- [7] Hu Lyuyang, Zheng Qunhua, Yu Feng, Chen Jingli, Luo Rong. Master Curve Drawing of Axial Transverse Dynamic Modulus Based on the Same Time-temperature Equivalent Factor. Journal of Wuhan University of Technology (Transportation Science & Engineering), 2019,43(01):146-152.
- [8] Fan Zhihong, Tang Guangxing, Deng Hongguan, Chang Mingfeng, Liu Hujun, Zhu Liang. Research on Dynamic Modulus Master Curve of Gneiss Modified Asphalt Mixture based on Time-Temperature Equivalence Principle. Highway, 2022, 67(12): 41-46.
- [9] Yin Yingmei, Zhang XiaoLing. Study on constitutive relation of asphalt mixtures based on dynamic creep test. Journal of Functional Materials, 2014, 45(23): 23020-23024.
- [10] Raza S M, Sharma K S. Optimizing porous asphalt mix design for permeability and air voids using response surface methodology and artificial neural networks. Construction and Building Materials, 2024, 442137513-137513.
- [11] Mahdi H, Ayman A, Daniel O, et al. Full-Scale Evaluation of Geosynthetic-Reinforced Hot Mix Asphalt. Transportation Research Record, 2023, 2677(9): 713-729.
- [12] Gou yuanyou, Li Yongle, Xiao Zilong, Liu Cuiran. Test and Study on Stress-Strain Relation of asphalt Concrete. Yellow River, 2005, (05):59-60+64.
- [13] Zheng Jianlong, Qian Guoping, Ying Ronghua. TESTING THERMALVISCOELASTIC CONSTITUTIVE RELATION OF ASPHALT MIXTURES AND ITS MECHANICAL APPLICATIONS. Engineering Mechanics, 2008, (01):34-41.
- [14] Wu Jinrong, Ma Qinyong. Experimental study on stress-strain relationship of asphalt mixtures. Subgrade Engineering, 2009, (02):66-67.

- [15] Pratap V W, Saurabh K, Ankit G. Identifying the Suitability of Warm Mix Asphalt for Reducing the Production Temperatures of Crumb Rubber–Modified Asphalt Mixtures: Economic and Environmental Perspective. Journal of Materials in Civil Engineering, 2024, 36(9):202-214
- [16] Wang Weibiao, Sun Zhentian, Wu Liyan. Study on stress-strain relationship of asphalt concrete. ShuiLi XueBao, 1996, (05):1-8+28.
- [17] Ye Xiangqian. Study on mechanical properties of thin overlay asphalt mixture based on discrete element method. Chongqing Jiaotong University, 2021.
- [18] Suleiman G, Aodah H H, Hanandeh S, et al. Investigating the Dynamic Creep of Polymer Modified Hot Mix Asphalt. Civil and Environmental Engineering, 2024, 20(1):387-396.
- [19] Wang Weibin, Wu Liyan. The Effects of Asphalt Contents on Stress-Strain Relations of Asphalt Concrete. Journal of Xi an University of Technology, 1995, (02):129-133+140.
- [20] Vaibhav K S, Neha S, Divas S, et al. Comparative evaluation of open graded friction course and stone matrix asphalt mixtures with modified binders and warm mix asphalt. Journal of Building Pathology and Rehabilitation, 2024, 9(2):98-115